https://doi.org/10.15255/KUI.2025.012
KUI-2/2026
Original scientific paper
Received February 22, 2025
Accepted April 16, 2025

Simultaneous Removal of Pb, Ni, Mn, and Cr from Phosphogypsum with Na_2EDTA: A Box-Behnken Design Modelling and Optimisation

E. Çelik[a,b*] and *S. Ertunç*[a]

[a] Ankara University, Department of Chemical Engineering, 06100 Ankara, Turkey
[b] Toros Agri Industry and Trade Co. Inc. R&D Center, 33 020 Mersin, Turkey

This work is licensed under a Creative Commons Attribution 4.0 International License

Abstract

Phosphogypsum (PG) is considered a by-product and is classified as solid waste generated during the production of phosphoric acid by the reaction of sulphuric acid with phosphate rock via the wet method. The presence of heavy metals in PG causes a range of environmental issues and poses limitations on its potential applications. In this study, the Box-Behnken design (BBD) technique was employed to simultaneously reduce concentrations of lead, nickel, manganese, and chromium in PG using Na_2EDTA. This approach aimed to optimise factors such as Na_2EDTA concentration, solid-to-liquid ratio (S/L), and contact time, while also developing a mathematical model. The optimal process points were identified through analysis of variance (ANOVA) and the response surface plots. Furthermore, the physicochemical properties of PG before and after purification were analysed using XRF, XRD, and FTIR methods. Based on the results obtained through response surface design methodology, the coefficients of correlation (R^2) of the experimental data and the second-order regression model for Pb, Ni, Mn, and Cr were found to be 89.75, 95.37, 98.18, and 94.53 %, respectively. Generally, high R-squared values indicate that the experimental data are consistent with the data predicted by the model under optimum conditions: $c(Na_2EDTA) = 0.055$ M, solid/liquid ratio = 1 : 20 g ml^{-1}, contact time = 157 min. Under these conditions, the removal efficiencies for Pb, Ni, Mn, and Cr were 46.65, 42.31, 67.02, and 77.9 %, respectively.

Keywords

Phosphogypsum, Na_2EDTA, removal of heavy metals, Box-Behnken experimental design

1 Introduction

Phosphogypsum (PG) is an acidic by-product residue produced in large volumes from the phosphatic fertiliser industry during the wet process for manufacturing phosphoric acid.[1] The chemical reaction is shown in Eq. (1).

$$Ca_5(PO_4)_3F + 5H_2SO_4 + 10H_2O \rightarrow \rightarrow 3H_3PO_4 + HF + 5CaSO_4 \cdot 2H_2O \quad (1)$$

In the wet process, depending on different reaction temperatures, phosphogypsum is generated in three different crystal structures: dihydrate ($CaSO_4 \cdot 2H_2O$), hemihydrate ($CaSO_4 \cdot 1/2H_2O$), and anhydrite $CaSO_4$.[1] The production of one metric ton of phosphoric acid (H_3PO_4) typically generates between 4.5 and 5.5 t of PG.[2,3] In Europe, PG production is estimated at 21 Mt/year, accumulated across approximately 30 sites, while global production ranges from 100–280 Mt *per* year.[4] Globally, only 14 % of PG is recycled, while 28 % is released into ecosystems, contaminating flora, fauna, and water sources, and 58 % is stored — often in ways that pose major environmental risks.[5] PG, which mainly comprises gypsum, also contains P_2O_5, fluorine, radionuclides (Ra, U, and Th), and significant levels of heavy metals such as Cd, As, Pb, Ag, Ba, and Cr,.[6] These elements appear on the Environmental Protection Agency's (EPA's) list of "Essential and Potentially Toxic Elements (PTEs)".[7] The use and storage of PG is a major concern for many countries due to its potential to cause water, soil, and air pollution.[8] There have been reports of land contamination, groundwater pollution, and crop contamination due to the presence of PG in many countries, such as Brazil, China, Greece, Jordan, Kazakhstan, Poland, Russia, Spain, Turkey, and USA.[9–11] Since PG waste is often transported and disposed of in slurry form, PG storage piles may be affected by tidal changes, and dissolution, and leaching of naturally occurring elements in PG can occur.[12]

In several countries, PG has long been evaluated in agriculture as a soil additive and fertiliser.[13] Recently, *Hentati et al.*[13] demonstrated that PG improved soil textural properties, calcium content, and quality of crop yield. However, *Nayak et al.*[14] noted possible negative effects on soil quality and nutrient security, and highlighted risks to human health through the food chain. Additionally, it was also indicated that heavy metals can accumulate in soil and food products, eventually posing serious health risks.[15] To address PG contamination, researchers have proposed various treatment methods, including water leaching, wet sieving, conversion to hemihydrate or anhydrite depending on temperature, neutralisation with bases such as ($Ca(OH)_2$, NH_4OH, …), or its effective treatment with acids such as sulphuric or citric acid.[16,17,7] *Jarosinski et al.*[18] investigated washing PG with an aqueous sulphuric acid solution to recover rare earth metals, and then manufacturing anhydrite from the purified PG by recrystallisation using sulphuric acid solution with a high molarity. Their results showed a

* Corresponding author: Ertuğrul Çelik, PhD (ORCID iD: 0000-0003-4837-4311), Email: ertugrulcelik88@gmail.com
Assoc. Prof. Suna Ertunç (ORCID iD: 0000-0002-0139-7463)

significant reduction in impurities, enabling the anhydrite to be used in plaster production.

Among the most important features that makes EDTA (ethylenediaminetetraacetic acid) a suitable option for removal of heavy metals are its low biodegradability, which allows it to retain metals for longer durations, its compatibility with various recycling methods, and it having minor effects on soil microbial and enzymatic activity compared to other agents, such as hydrochloric acid.[19–21] Chelators like EDTA typically remove metals from soil through the desorption-complexation-dissolution process. EDTA has the ability to rapidly dissociate some unstable chain bonds between heavy metals and soil particles, and the dissolution of the resulting metal-EDTA complexes may further weaken the metal-oxygen bonds within its structure forming soluble metal-EDTA complexes that retain the heavy metals within the solution.[22] In earlier surveys, scientists have commonly used EDTA to remove heavy metals from sludge, cathode ray tube waste, and contaminated surfaces like soils.[23–27] In general, most EDTA is denoted by the free acid (H_4Y) and the disodium salt is $Na_2H_2Y{\cdot}2H_2O$ form. H_4Y has a very low solubility in water, and therefore the disodium salt $Na_2H_2Y{\cdot}2H_2O$, in which two of the acid groups are neutralised, is generally used when preparing the solution.[28] Disodium ethylenediaminetetraacetate is a widely used chelating agent in both laboratories and industrial settings.[29] The molecular structures of EDTA complexes and the disodium EDTA salt are presented in Fig. 1.

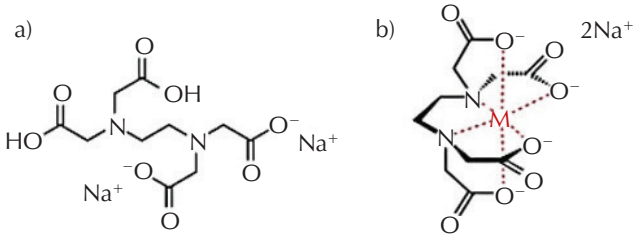

Fig. 1 – Structures of (a) EDTA disodium salt, and (b) metal–EDTA complexes

It is highly desirable to investigate multivariate statistical solutions for optimising the experimental model parameters. The Box-Behnken design (BBD), a key method within response surface methodology (RSM), is one of the most widely applied multivariate statistical tools for optimising operational parameters and various processes. This method involves multiple regression analysis, diagnostic testing using analysis of variance (ANOVA), and fitting a polynomial equation to account for all possible parameter combinations and to understand their impact on the desired responses. The primary advantage is to gain essential information and identify the logical optimal experimental conditions for target responses while requiring fewer experimental runs.[30] Additionally, BBD offers cost and time efficiency, with high accuracy in identifying the effects of interactions among one or more independent variables and the estimated responses. It is especially effective in the general optimisation processes, helping to minimise costs and avoid running experiments under extreme conditions.[31,32]

The aim of this study was to evaluate the simultaneous removal of manganese, nickel, lead, and chromium from PG using $Na_2H_2Y{\cdot}2H_2O$, through the application of response surface methodology. In addition, this study aimed to optimise parameters such as Na_2EDTA concentration, solid-to-liquid ratio, and contact time for simultaneous reduction of manganese, nickel, lead, and chromium from PG using the RSM's Box-Behnken Design.

2 Materials and methods

2.1 Materials

The PG samples used in this study were obtained from a fertiliser manufacturer in Turkey. To ensure representativeness, samples were collected from at least 10 different locations and mixed. Initially, the PG was dried for 48 h at 100 °C. Using an automatic vibratory sieve (Retsch), the dried samples were sieved by a 38 μm < PG < 75 μm particle size sieve. The heavy metal content before purification of phosphogypsum are shown in Table 1. The following materials and equipment were used in this study: Na_2EDTA (AnalaR-BHD Chemical) as chelating agent for removal of heavy metals, H_2SO_4 (Sigma Aldrich) for the recovery of Na_2EDTA by precipitation, analytical balance (Radwag AS 220/C/2) for weighing samples, magnetic stirrer (Wisestir MSH-20A) for mixing, and oven (Thermomac FCD-3000 Serials) for the drying process.

Table 1 – Major potentially toxic elements found in PG

Element	As	Cd	Co	Cu	Hg	Ni	Mn	Pb	Cr
Content / mg kg^{-1}	0.4	0.9	5.5	0.7	0.7	5.0	15.5	5.8	14.0

Actually, the elemental composition of PG varies depending on its ingredient in the natural phosphate ore and the manufacturing process used.[33]

2.2 Purification method of PG

For the batch leaching experiments, three different concentrations of Na_2EDTA (0.001, 0.005, and 0.01 M) were used to reduce the concentrations of Pb, Ni, Mn, and Cr in PG. Deionised water was used to prepare the solution at the specified concentrations. The experiments were conducted at room temperature, with a mixing speed of 170 rpm, and solid-to-liquid ratios of 1 : 10, 1 : 15, and 1 : 20. Contact times were set at 60, 120, and 180 min. The filtered solids were dried in an oven at 50 °C overnight. The percentages of Pb, Ni, Mn, and Cr removal efficiencies (R) were assessed using Eq. (2).

$$R, \text{Metal } [\%] = ((c_i - c_f)/c_i) \cdot 100 \quad (2)$$

R is the coefficient of correlation, c_i is the initial heavy metal concentration as mg kg^{-1} in PG, and c_f is the final heavy metal concentration after the purification process.

2.3 Experimental design for optimum working conditions

The concentration of Na_2EDTA, contact time, and solid-to-liquid ratio were optimised using the Box-Behnken design (BBD) to determine both the main and interaction effects on the percentage removal of Pb, Ni, Mn, and Cr. The BBD experimental design was conducted by evaluating ANOVA via the Design Expert 12.0.3 software. The Box-Behnken design was employed to optimise the removal process with three factors: Na_2EDTA concentration, contact time, and solid-to-liquid ratio. BBD was constructed using real and coded values in different levels and three independent variables (−1, 0, +1) as shown in Table 2. Each independent variable was coded according to Eq. (3).

$$x_i = (D_i - D_0)/\Delta D_i \quad (3)$$

where x_i is the dimensionless value of the variable, D_i is the real value of the variable, D_0 is the real value of the variable at the centre point, and ΔD_i is the step change.[34]

Table 2 – Three selected independent variables and levels of the Box-Behnken design

		Level		
		Low	Central	High
Factor	Symbol	−1	0	+1
Na_2EDTA / mol l^{-1}	A	0.001	0.05	0.1
Solid/liquid / g ml^{-1}	B	1 : 10	1 : 15	1 : 20
Contact time / min	C	60	120	180

Here, the concentration of Na_2EDTA (mol l^{-1}), solid-to-liquid ratio (g ml^{-1}), and contact time (min) are the independent input parameters. Moreover, the number of experiments required for the BBD was determined using Eq. (4):

$$\text{experiment number} = 2k(k-1) + c_0 \quad (4)$$

where k is the number of variables, and c_0 is the number of centre points.[35] A total of 17 experimental runs were performed for the three-level, three-factor Box-Behnken experimental design. The centre points helped to measure the pure error of the curvature.[36]

A quadratic polynomial model was applied to analyse and predict the efficiency of heavy metal removal, as shown in Eq. (5).

$$Y = \beta_0 + \sum \beta_i X_i + \sum \beta_{ii} X_i^2 + \sum\sum \beta_{ij} X_i X_j \quad (5)$$

Y is the predicted response (extraction recovery) and X_i and X_j are the independent variables (Na_2EDTA concentration, solid-to-liquid ratio, and contact time) that are known for each experimental run. The parameter β_0 is the model constant, β_i is the first-order main effect, β_{ii}s are the quadratic coefficients, and β_{ij}s are the interaction coefficients.[37]

The model quality was assessed by analysis of variance (ANOVA), based on the coefficient of correlation (R^2), probability value (p-value), and the F-value (Fisher method). Response surface methodology (RSM) plots were generated to aid in the optimisation of the processes.

2.4 Characterisation and analysis method

X-ray diffraction (XRD) patterns were obtained using an Inel brand Equinox 1000 model X-Ray Diffractometer (XRD) device operated at 30 mA and 30 kV, equipped with a cobalt (Co) anode. To identify the elemental composition of PG, X-ray fluorescence analysis was performed using a polarised energy dispersive X-ray fluorescence spectrometer (SPECTRO XLAB 2000) fitted with a 400 W Rh end window tube and a Si(Li) detector with a resolution of 148 eV (1000 cps Mn Ka). Fourier transform infrared spectroscopy (FTIR) analysis was used to investigate the composition of the products was performed using a Shimadzu FTIR-8400 spectrophotometer. Each sample (0.001 g) was mixed with 0.1 g of pure KBr, ground uniformly, placed into a mould and then pressed into a transparent thin sheet using a hydraulic press, and scanned across the range of 400–4000 cm^{-1}.

3 Results and discussion

3.1 Optimisation of parameters with Box-Bhenken design

To evaluate the combined effect of the three selected parameters on the removal of Pb, Ni, Mn, and Cr, the RSM based on BBD was employed to determine the optimal values. All removal experiments were conducted in triplicate, and the average values were reported. The experiments were designed as shown in Table 3.

3.2 Variance analysis

The accuracy and validity of the model can be assessed using the F-value and p-value. The p-value for each independent variable is used to determine the level of statistical significance of each variable related to the dependent variable. A higher F-value indicates better conformance of the model with the experimental data. A low p-value (< 0.05) and a high F-value (> 1) suggest a better fit of the experimental data to the model results. The coefficient of regression (R^2) is employed to express the degree of compatibility between experimental data and model results. Generally, the R^2 values range from 0 to 1, and an R^2 value greater than 0.80 is considered indicative of a reasonable fitting between experimental and predicted values.[38]

ANOVA is a collection of statistical models used to analyse how independent variables interact with each other and

Table 3 – Box-Behnken experimental design with three independent variables

Run	A: Na_2EDTA /M	B: Solid-to-liquid / g ml^{-1}	C: Contact time /min	Pb removal /%	Ni removal /%	Mn removal /%	Cr removal /%
1	0.0505	1 : 15	120	46.23	43.36	56.22	79.26
2	0.0505	1 : 15	120	45.25	46.66	59.12	80.12
3	0.0505	1 : 10	60	44.36	40.02	58.26	80.74
4	0.1	1 : 10	120	48.27	35.00	30.23	62.26
5	0.1	1 : 15	180	49.26	33.26	35.26	68.63
6	0.001	1 : 15	180	31.03	45.26	20.56	48.45
7	0.1	1 : 15	60	51.72	32.56	36.56	61.23
8	0.001	1 : 15	60	36.30	42.56	20.79	44.32
9	0.0505	1 : 10	180	46.55	42.82	62.21	78.23
10	0.0505	1 : 20	180	46.92	43.45	74.25	75.27
11	0.0505	1 : 15	120	51.72	41.66	62.23	72.23
12	0.0505	1 : 20	60	44.20	43.33	56.23	78.12
13	0.1	1 : 20	120	48.26	33.33	33.23	69.12
14	0.001	1 : 10	120	36.20	51.66	19.23	43.79
15	0.0505	1 : 15	120	46.25	43.26	61.36	70.01
16	0.0505	1 : 15	120	46.55	42.33	60.22	69.79
17	0.001	1 : 20	120	36.20	41.66	20.78	42.20

the effects of these interactions on the dependent variable.[39] In this study, three separate regression models were developed for the removal of Pb, Ni, Mn, and Cr from PG. Statistical testing of the regression equations were controlled with the F test, and the fit of the model was evaluated through quadratic ANOVA. The ANOVA results are shown in Table 4.

Low *p*-values of the model are 0.0096, 0.0007, < 0.0001, and 0.0012 for Pb Ni, Mn, and Cr, respectively. The *p*-value of 0.05 or lower is commonly considered a statistically significant result.[40] Additionally, the high *F*-values for Pb (6.81), Ni (16.03), Mn (41.95), and Cr (13.45) further confirmed the significance of the model. The sum of square values associated with Na_2EDTA concentration effect was high for Pb (417.32), Ni (569.03), Mn (363.42), and Cr (850.37), indicating that Na_2EDTA concentration had the most significant effect on the heavy metal removal. Solid-to-liquid ratios and contact times exhibited relatively lower mean square values, suggesting a less significant impact on heavy metal removal.

As shown in Table 4, the high *F*-value, low *p*-values, and sum of squares values obtained for the model authenticity indicated that the model was significant.

Table 4 – ANOVA results of quadratic models

Source	Sum of squares	df	Mean square	*F*-value	*p*-value	
Pb removal/%						
Model	504.71	9	56.08	6.81	0.0096	significant
A – Na_2EDTA	417.32	1	417.32	50.69	0.0002	
B – solid-to-liquid	0.0050	1	0.0050	0.0006	0.9810	
C – contact time	0.9941	1	0.9941	0.1208	0.7384	
AB	0.0000	1	0.0000	3.037E-06	0.9987	
AC	1.97	1	1.97	0.2398	0.6393	
BC	0.0702	1	0.0702	0.0085	0.9290	
A^2	74.16	1	74.16	9.01	0.0199	
B^2	2.48	1	2.48	0.3007	0.6005	

Table 4 – (continued)

Source	Sum of squares	df	Mean square	*F*-value	*p*-value	
C^2	3.58	1	3.58	0.4346	0.5308	
Residual	57.62	7	8.23			
Lack of fit	31.31	3	10.44	1.59	0.3252	not significant
Pure error	26.32	4	6.58			
Total	562.33	16				
R^2 = 0.8975, R^2 (adjusted) = 0.8358, R^2 (predicted) = 0.5861, Adeq Precision = 11.2028						
Ni removal/%						
Model	622.29	9	69.14	16.03	0.0007	significant
A – Na_2EDTA	569.03	1	569.03	131.94	0.0003	
B – solid-to-liquid	0.2278	1	0.2278	0.0528	0.8248	
C – contact time	0.1984	1	0.1984	0.0460	0.8363	
AB	1.53	1	1.53	0.3537	0.5708	
AC	9.86	1	9.86	2.29	0.1743	
BC	1.80	1	1.80	0.4163	0.5393	
A^2	21.57	1	21.57	5.00	0.0604	
B^2	2.81	1	2.81	0.6513	0.4462	
C^2	14.66	1	14.66	3.40	0.1078	
Residual	30.19	7	4.31			
Lack of fit	15.38	3	5.13	1.39	0.3687	not significant
Pure error	14.81	4	3.70			
Total	652.48	16				
R^2 = 0.9537, R^2 (adjusted) = 0.8942, R^2 (predicted) = 0.6873, Adeq Precision = 13.6405						
Mn removal/%						
Model	5431.16	9	603.46	41.95	< 0.0001	significant
A – Na_2EDTA	363.42	1	363.42	25.26	0.0015	
B – solid-to-liquid	26.50	1	26.50	1.84	0.2169	
C – contact time	52.22	1	52.22	3.63	0.0984	
AB	0.5256	1	0.5256	0.0365	0.8538	
AC	0.2862	1	0.2862	0.0199	0.8918	
BC	49.49	1	49.49	3.44	0.1060	
A^2	4925.88	1	4925.88	342.39	< 0.0001	
B^2	0.2451	1	0.2451	0.0170	0.8998	
C^2	29.93	1	29.93	2.08	0.1924	
Residual	100.71	7	14.39			
Lack of fit	78.92	3	26.31	4.83	0.0812	not significant
Pure error	21.79	4	5.45			
Total	5531.87	16				
R^2 = 0.9818, R^2 (adjusted) = 0.9584, R^2 (predicted) = 0.7656, Adeq Precision = 18.2050						
Cr removal/%						
Model	2774.60	9	308.29	13.45	0.0012	significant
A – Na_2EDTA	850.37	1	850.37	37.09	0.0005	

Table 4 – (continued)

Source	Sum of squares	df	Mean square	*F*-value	*p*-value	
B – solid-to-liquid	0.0120	1	0.0120	0.0005	0.9824	
C – contact time	4.76	1	4.76	0.2076	0.6625	
AB	17.85	1	17.85	0.7786	0.4068	
AC	2.67	1	2.67	0.1166	0.7428	
BC	0.0289	1	0.0289	0.0013	0.9727	
A^2	1889.88	1	1889.88	82.43	< 0.0001	
B^2	6.54	1	6.54	0.2854	0.6098	
C^2	27.63	1	27.63	1.20	0.3086	
Residual	160.49	7	22.93			
Lack of fit	58.99	3	19.66	0.7748	0.5658	not significant
Pure error	101.50	4	25.38			
Total	2935.08	16				
R^2 = 0.9453, R^2 (adjusted) = 0.8750, R^2 (predicted) = 0.6244, Adeq Precision = 10.1035						

The lack of fit test was conducted to evaluate the adequacy of the model. The lack of fit *F*-values for Pb, Ni, Mn, and Cr were 1.59, 1.39, 4.83, and 0.77, respectively. These values were determined to be insignificant for all four treatments, as the *p*-values for lack of fit were ≥ 0.05 in each case. The lack of fit test due to pure error is insignificant and the non-significance of this term indicates the accuracy of the model.[41] Additionally, the insignificance of the lack of fit value is an indicator of the model's strong predictive performance.[35]

The regression coefficients (R^2) obtained for each metal were: Pb (0.8975), Ni (0.9537), Mn (0.9818), and Cr (0.9453), indicating that Pb (0.1025 %), Ni (0.0463 %), Mn (0.0182 %), and Cr (0.0547 %) were not sufficiently described by the model due to error. Statistical analysis of the regression model revealed a low correlation for Pb removal, suggesting that this process negatively affects both the linear and quadratic model by the Na_2EDTA concentration.

The adjusted R^2 and predicted R^2 values of the model were as follows: Pb (0.8358–0.5861), Ni (0.8942–0.6873), Mn (0.9584–0.7656), and Cr (0.8750–0.6244). The adjusted and predicted R^2 valuesujjuui87 for the four elements were in reasonable conformity, indicating this quadratic model's adequacy for predicting the best possible values of factors at maximum simultaneous extraction of Pb, Ni, Mn, and Cr.

Adeq precision values were also found to be high. This metric, which measures the signal-to-noise ratio, should exceed 4 for a desirable model 4.[42] The obtained ratios were 11.2028, 13.6405, 18.2050, and 10.1035 for Pb, Ni, Mn, and Cr, respectively, confirming that the model provides an appropriate and adequate signal, and can be reliably used to study and create the design space.

For the linear model, the adjusted and predicted R^2 values were low, although the *p*-value of Pb removal was significant. Nevertheless, removal of Pb was still observed. These findings indicate that the model obtained is valid for the experimental study. Although the *p*-value of Pb removal was significant, the adjusted R^2 and predicted R^2 values were low for the linear model.

3.3 Mathematical model fitting

The four empirical models were derived from both experimental data and quadratic polynomial equations. To analyse the empirical relationship between the predicted removal efficiencies of heavy metals and the effective variables, *i.e.*, the combined effects of *A* (Na_2EDTA concentration), *B* (solid-to-liquid ratio), and *C* (contact time), the quadratic polynomial equations were expressed as Eqs. (6–9).

$$\text{Pb removal } (Y_1) = 47.20 + 7.22A + 0.0250B - 0.3525C - 0.0025AB + 0.7025AC + 0.1325BC - 4.20A^2 - 0.7688B^2 - 0.9237C^2 \quad (6)$$

$$\text{Ni removal } (Y_2) = 43.45 - 5.87A - 0.9662B + 0.7900C + 2.08AB - 0.500AC - 0.6700BC - 3.52A^2 + 0.4767B^2 - 1.53C^2 \quad (7)$$

$$\text{Mn removal } (Y_3) = 59.83 + 6.74A + 1.82B + 2.56C + 0.3625AB - 0.2675AC + 3.52BC - 34.20A^2 + 0.2413B^2 + 2.67C^2 \quad (8)$$

$$\text{Cr removal } (Y_4) = 74.28 + 10.31A - 0.0388B + 0.771C + 2.11AB + 0.8175AC - 0.0850BC - 21.19A^2 + 1.25B^2 + 2.56C^2 \quad (9)$$

In the case of Mn, Ni, Pb, and Cr removal, *A, B, C, AB, AC, BC,* A^2, B^2, and C^2 would be our significant model terms.

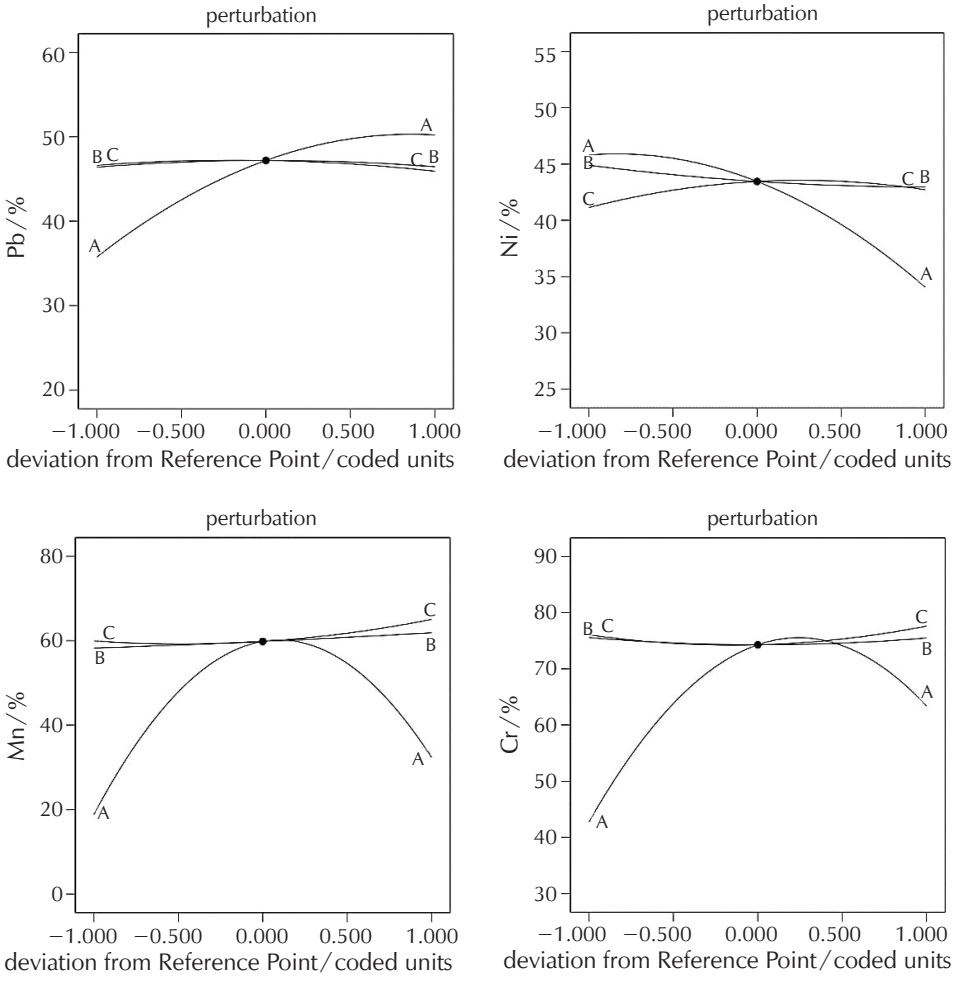

Fig. 2 – Perturbation plots for % removal efficiency of Pb, Ni, Mn, and Cr

3.4 Analysis of residual plots

The comparative effects of all independent variables on the removal efficiency of Pb, Ni, Mn, and Cr with the perturbation plot is shown in Fig. 2.

The Na_2EDTA concentration showed a sharp curvature (parameter *A*), indicating that the removal efficiency of Pb, Ni, Mn, Cr was highly responsive to this factor. The curves for solid-to-liquid ratio (*B*) and contact time (*C*) were less responsive for Pb, Ni, Mn, Cr removal efficiency. In addition, the Na_2EDTA concentration term in the quadratic model exhibited statistical significance for Pb (0.0002), Ni (0.0003), Mn (0.0015), and Cr (0.0005), with all *p*-values being less than $p < 0.01$. These low *p*-values indicate a strong relationship between Na_2EDTA concentration and the optimisation of the removal process for each of these metals. The normal probability plot shown in Fig. 3 was used to assess the assumption of normality for the residuals. The alignment of the data points with the reference line indicates that the residuals conform to an approximately normal distribution. In a normally distributed dataset, residuals are expected to lie along a straight diagonal line in the probability plot.[43] Although minor deviations are present, they exhibit no systematic pattern. Moreover, the residuals appear to be randomly scattered above and below the reference line, further supporting the validity of the normality assumption.

The performance and adequacy of the model were assessed by examining the plot of predicted values against the actual (observed) values, as shown in Fig. 4. The close alignment of the data points along the 45-degree reference line suggests a strong agreement between predicted and actual values, indicating that the quadratic regression model provides a satisfactory fit to the data. This linear pattern implies minimal deviation between predictions and observations. Furthermore, the residuals display random dispersion and symmetry around the regression line, which supports the assumptions of normality and independence. These characteristics validate the underlying assumptions of the model.[44]

It has been shown that the predicted values and experimental data are in perfect conformity with each other and the resulting response surface model fits well with the regression model, which demonstrates its adequacy for successful prediction of Mn, Cr, Ni and Pb removal. This

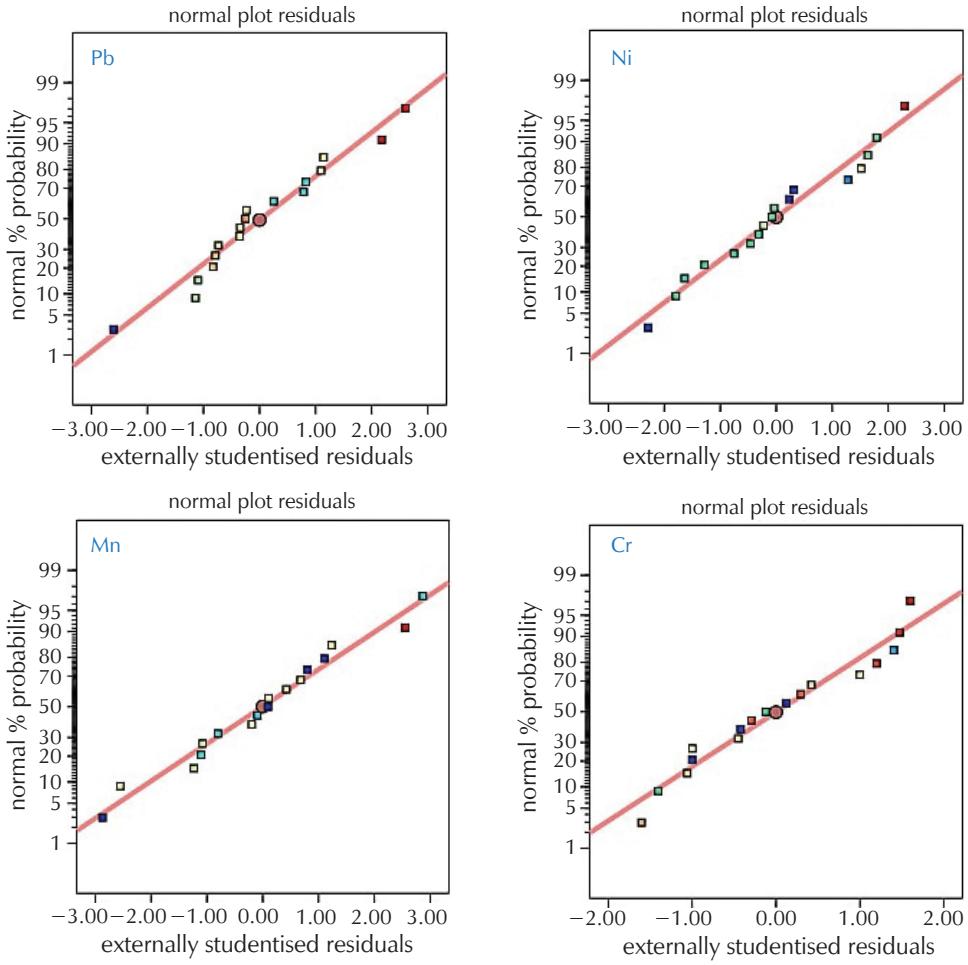

Fig. 3 – Normal probability plots of residuals

observation indicated that the experimental results for this study are quite admissible. Moreover, the R^2 value being greater than 0.80 is adequate to verify the suitability between the experimental and predicted values.[45]

The scatter plots shown in Fig. 5 offer information about the distribution of residuals, which is critical for assessing the optimisation of the model. The residuals appear to be randomly scattered around the zero line, with no discernible patterns or systematic structure. This observation supports the assumption of homoscedasticity, indicating that the residuals exhibit constant variance across the range of fitted values. Moreover, the predicted removal efficiencies for Pb (31.03–51.72 %), Ni (32.56–51.66 %), Mn (19.00–74.25 %), and Cr (42.20–80.74 %) lie within the admissible experimental ranges. This outcome confirms that the model is both suitable for optimisation and reliable in predicting removal efficiencies.

3.5 Response surface plots

Three-dimensional (3D) response surface plots, which are graphical diagrams of regression equations, were used to show the mutual influence of two factors while all other factors were held at constant levels.[46] Analysis of the plotted response surfaces allows identification of areas where the tested input parameters mutually produced the most advantageous response.[47] The 3D surface plots showed that *A* (Na_2EDTA concentration), *B* (solid-to-liquid ratio), and *C* (contact time) were important variables to achieve high removal percentage.

Fig. 6 shows the relationship of Na_2EDTA concentration and solid-to-liquid ratio on the removal efficiency of Pb, Ni, Mn, and Cr elements. At this point, the contact time was kept constant at 120 min. The removal efficiency of Mn was reduced from 20.78 to 19.23 % with a decrease in the solid-to-liquid ratio of Pb, Ni, Mn, and Cr from 1 : 20 to 1 : 10 g ml^{-1}, while the removal efficiencies were increased for Ni from 50.25 to 51.66 %, and for Cr from 42.2 to 43.79 %, and a linear effect was noticed for Pb. The removal efficiencies were increased for Pb from 36.2 to 48.26 %, for Ni from 31.12 to 50.25 % with an increase in the Na_2EDTA concentration in Pb, Ni, Mn, and Cr experiments from 0.001 to 0.1 M, while the removal efficiency of Mn decreased from 33.23 to 20.78 % and for Cr from 69.12 to 42.2 %.

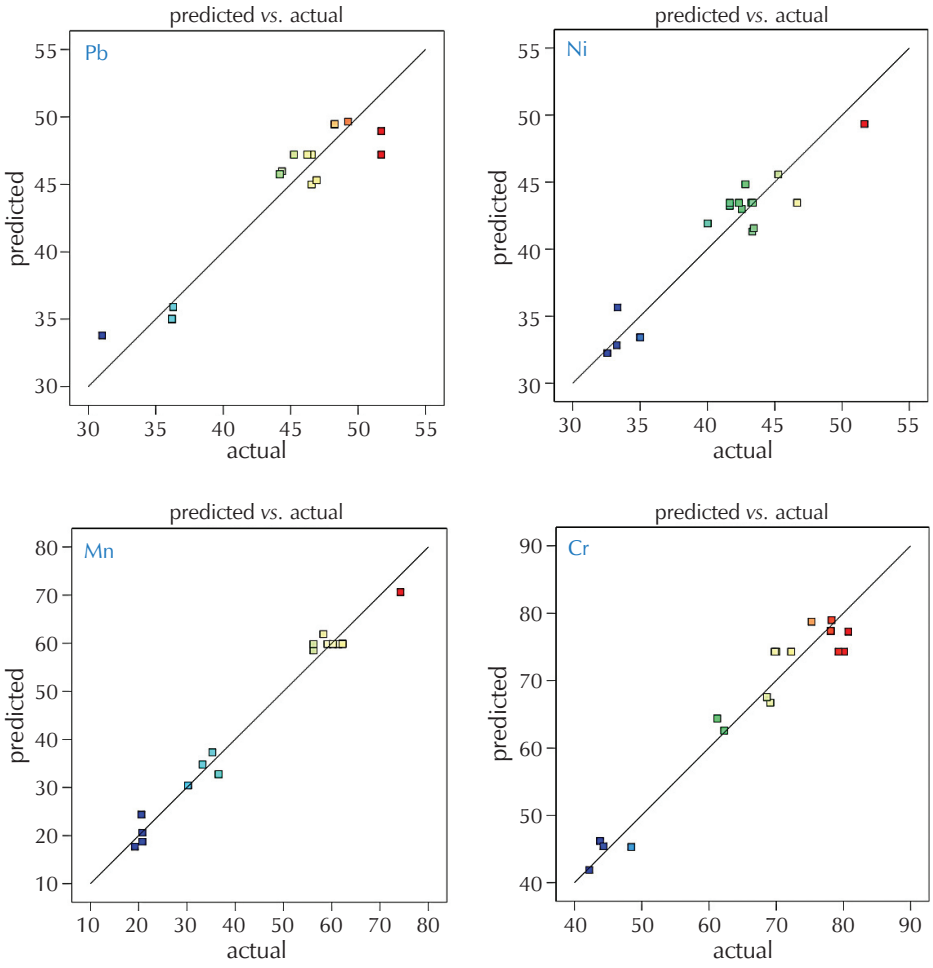

Fig. 4 – Plots of element removal % for actual and predicted results

Fig. 7 shows the interaction between Na_2EDTA concentration and contact time for Pb, Ni, Mn, and Cr elements, and their impact on the removal efficiency. At this point, the solid-to-liquid ratio was kept constant at 1 : 15 g ml^{-1}. The removal efficiency of Cr was decreased from 48.45 to 44.32 % by decreasing the contact time from 180 to 60 min, while the removal efficiency was increased for Pb from 31.03 to 36.3 % and from 45.26 to 49.23 % for Ni, a linear effect is shown for Mn. The removal efficiency increased for Pb from 31.03 to 49.26 %, for Mn from 20.56 to 35.26 %, and for Cr from 48.45 to 68.63 % with an increase in the Na_2EDTA concentration of Pb, Ni, Mn, and Cr from 0.001 to 0.1 M, while the removal efficiency of Ni decreased from 45.26 to 32.56 %.

Fig. 8 shows the effect of interaction of solid-to-liquid ratio and contact time on the removal efficiency of Pb Ni, Mn, and Cr elements. At this point, the Na_2EDTA concentration was kept constant at 0.05 M. The removal efficiency of Pb, Ni, Mn, and Cr shows a linear effect between the solid-to-liquid ratio (1 : 10–1 : 20 g ml^{-1}) and time (60–180) min. A higher extraction efficiency was obtained with the increase in the solid-to-liquid ratio over time.

3.6 Confirmation of the optimum model

This step was performed to determine the optimum values of process variables such as Na_2EDTA concentration, solid-to-liquid ratio, and contact time for simultaneous removal of lead, nickel, manganese, and chromium by applying the models derived from experimental results. The optimal reaction conditions and corresponding predictive values for the independent variables are as follows: Na_2EDTA concentration of 0.055 M, solid-to-liquid ratio of 1 : 20 g ml^{-1}, and contact time of 157 min.

These independent variables are common values across all tested process parameters. Under optimal conditions, the model predicted removal efficiencies for Pb, Ni, Mn, and Cr of 46.63, 42.29, 67.04, and 77.92 %, respectively. To verify the accuracy of the model, additional experiments were conducted under optimal conditions. The actual removal efficiencies obtained in the experimental study were Pb (46.65 ± 0.02 %), Ni (42.31 ± 0.02 %), Mn (67.02 ± 0.02 %), and Cr (77.9 ± 0.02 %). This confirmed sufficient consistency between the actual value and the predicted values ($p > 0.05$).[42]

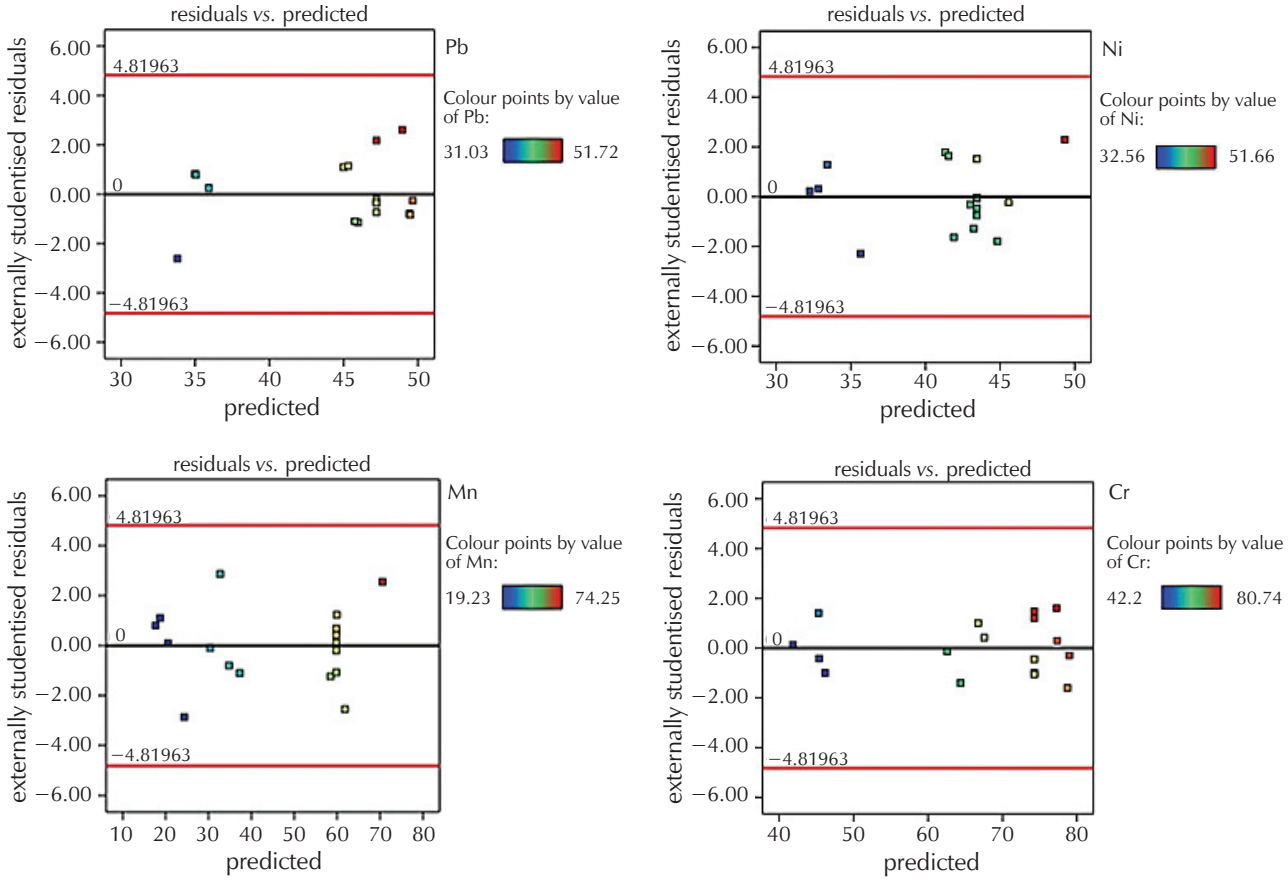

Fig. 5 – BBD results for percent removal of elements

3.7 X-Ray fluorescence (XRF) analysis

According to the XRF analysis, the removal efficiencies of Mn, Ni, Pb, and Cr from PG under optimal conditions indicated a significant reduction in heavy metal content. Among the studied metals, Cr exhibited the highest removal efficiency of 77.9 %, reducing its concentration from 14.0 to 3.09 ppm. This was followed by Mn with a 67.02 % reduction (from 15.5 to 5.11 ppm), Pb with 46.65 % (from 5.8 to 3.09 ppm), and Ni with 42.31 % (from 5.0 to 2.88 ppm).

These results demonstrate the effectiveness of the applied purification method under optimal conditions, particularly in the removal of Cr and Mn, which are typically more persistent in industrial waste materials. The substantial reduction in heavy metal content suggests that the treated PG may have reduced environmental risks and may be more suitable for reuse or safer disposal.

3.8 Fourier transform infrared spectroscopy (FTIR) analysis

In order to investigate the preservation of the structure of PG during the application of Na_2EDTA at different concentrations, the FTIR analysis spectra of phosphogypsum before and after purification, corresponding to the maximum removal of Pb, Cr, Ni, and Mn, are given in Fig. 9.

The fundamental vibrational modes of phosphogypsum were assigned to the peaks in FTIR spectra. The peaks observed at approximately 3556 and 3402 cm^{-1} are attributed to O−H stretching vibrations of the crystallised water in PG. The peaks at approximately 1689 and 1620 cm^{-1} are characteristic of the O−H bending vibrations of the crystallised water. Two bands at 601 and 671 cm^{-1} are attributed to the asymmetric vibration mode of SO_4^{2-}. Overall, FTIR peaks are consistent with those reported in previous studies.[48] These findings clearly indicate that Na_2EDTA is suitable for purifying PG solid waste containing Mn, Ni, Cr, and Pb contamination.

3.9 X-ray Diffraction (XRD) analysis

The morphological crystallinity alteration in phosphogypsum phase in 2 steps (before and after) purification and the maximum removal for Pb, Cr, Ni, and Mn are given in Fig. 10.

The XRD pattern shows that the main component of the PG sample was gypsum ($CaSO_4 \cdot 2H_2O$) with a small amount of brushite ($CaHPO_4 \cdot 2H_2O$) and quartz (SiO_2). In the XRD analysis performed after the use of Na_2EDTA, it was determined that the calcium sulphate dihydrate, silica, and calcium phosphate phases in the phosphogypsum were dissoluted.[49]

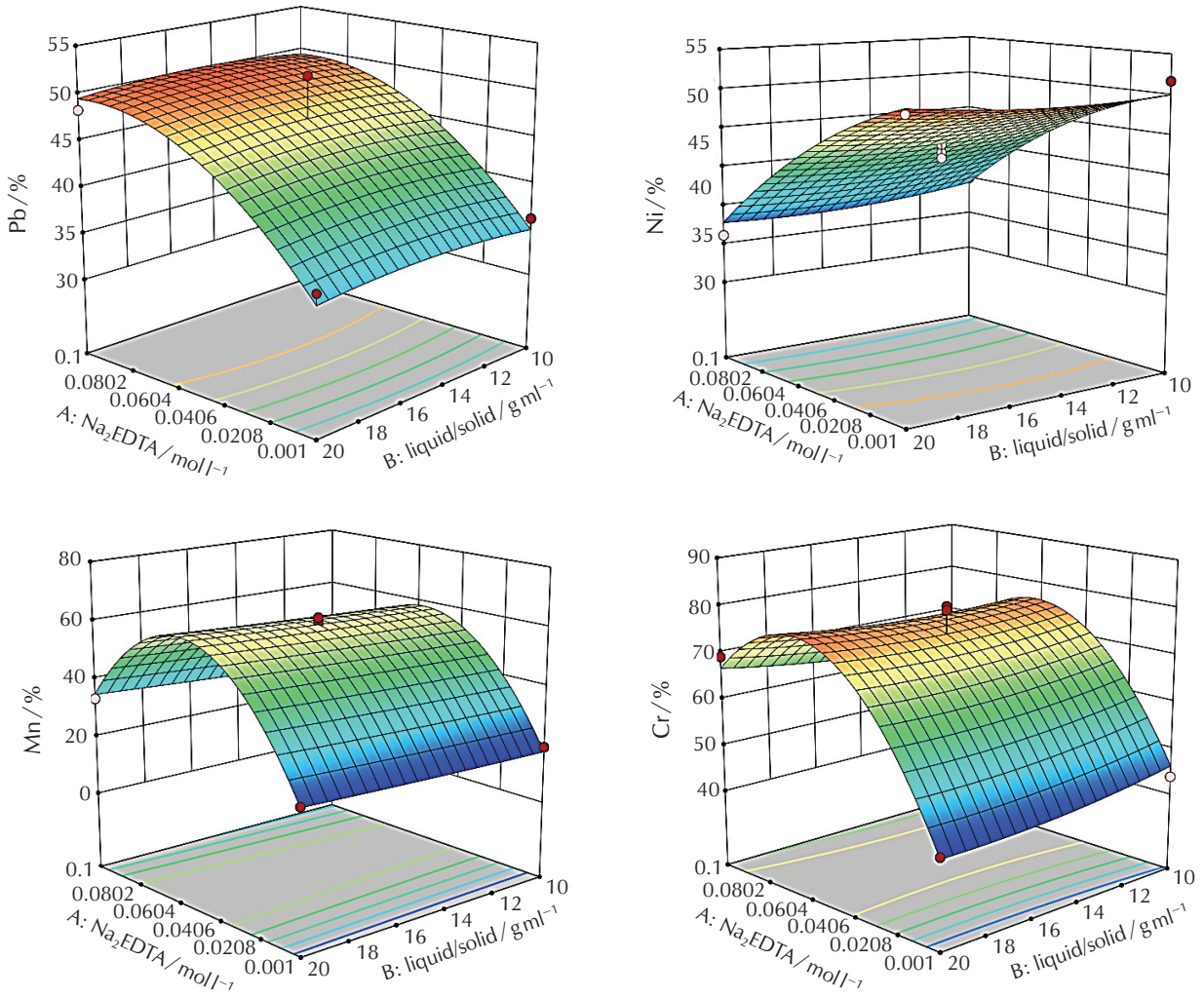

Fig. 6 – Response surface plots of Na_2EDTA concentration and solid-to-liquid ratio

3.10 Recoverability of Na_2EDTA

Due to the poor biodegradability of EDTA, its persistence and mobilisation in the environment may lead to adverse ecological effects including impacts on soil aggregate stability and water retention properties.[50,51] Various studies have proposed different procedures for recovering EDTA from the heavy metal– EDTA complexes after the extraction procedure. As a significant amount of authentic EDTA remains in the aqueous solution after the removal procedure, recovering and reusing this chelating agent is economically beneficial.[52] Faster precipitation of EDTA can be achieved using low concentrations of sulphuric acid.[53]

The pH-value of the solution after the extraction process was measured at 4.69 and was subsequently reduced to 2.0 by adding sulphuric acid drop by drop using the precipitation method. After filtration, the Na_2EDTA remaining on the filter paper was rinsed once with distilled water and dried in an oven at 50 °C overnight. In this study, 71.4 % of the Na_2EDTA was successfully recovered. The FTIR spectra of both fresh Na_2EDTA and Na_2EDTA recovered by precipitation are shown in Fig. 11.

The infrared spectrum of fresh Na_2EDTA and first-time recycled Na_2EDTA showed similar bands. The region between 3600–3000 cm^{-1} (3518, 3402, 3387, 3032, and 3016) corresponds to hydroxyl groups due to O−H and N−H stretching vibration. The vibrational bands located near 2700–2500 cm^{-1} (2669 and 2584) are characteristic of formation of dimers for carboxylic acid and are attributed to the C−O stretching and O−H bending absorption modes. The bands at 1681 and 1627 cm^{-1} are related to carboxylic groups. The peaks observed at 1481 and 1419 cm^{-1} are associated with the symmetrical carboxyl stretching, while the bands at 1396, 1319, and 1311 cm^{-1} are also attributed to carboxyl groups. The absorption bands between 900–700 cm^{-1} (771 and 709) originate from C−H stretching and bending vibrations. These data are consistent with previous studies.[53,54]

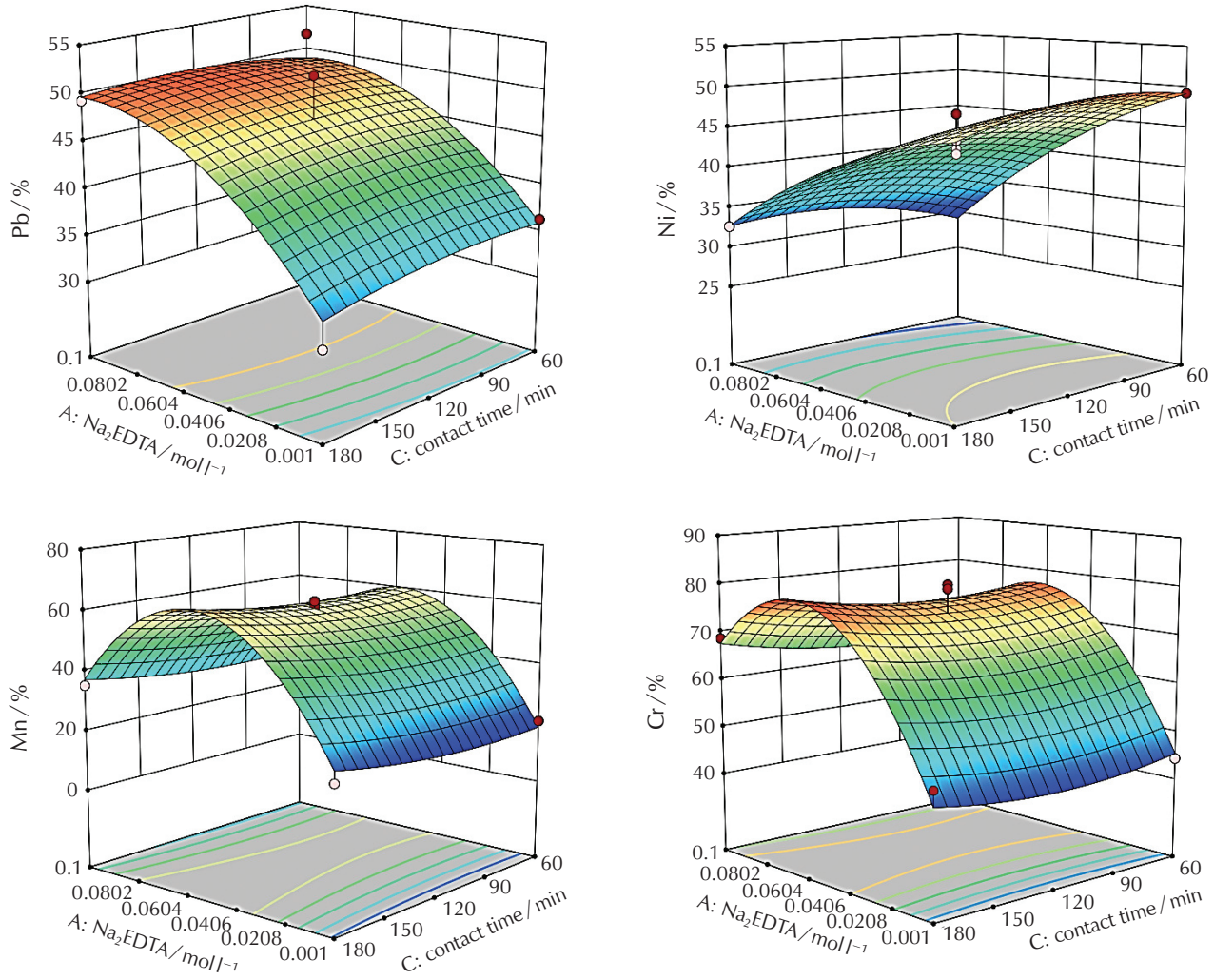

Fig. 7 – Response surface plots of Na_2EDTA concentration and contact time

4 Conclusions

This study comprehensively evaluated the simultaneous removal of heavy metals (Pb, Ni, Mn, and Cr) from PG using Na_2EDTA as a chelating agent. In addition, the optimisation of key operational parameters was investigated, and the resulting structural and chemical modifications within the PG matrix were examined.

Through experimental modelling, the optimised parameters for maximum metal removal were determined to be a solid-to-liquid ratio of 1 : 20 g ml^{-1}, a contact time of 157 min, and a Na_2EDTA concentration of 0.055 M. These optimised parameters were common across all tested heavy metals, indicating a unified approach for multi-metal removal from PG. The model-predicted removal efficiencies for Ni, Pb, Mn, and Cr were 42.29, 46.63, 67.04, and 77.92 %, respectively. Subsequent validation experiments conducted under these conditions yielded actual removal rates of 42.31 ± 0.02, 46.65 ± 0.02, 67.02 ± 0.02, and 77.90 ± 0.02 % for Ni, Pb, Mn, and Cr, respectively.

The strong agreement between predicted and experimental values ($p > 0.05$) confirms the accuracy and reliability of the developed model for predicting and optimising the removal of heavy metals from PG using Na_2EDTA.

X-ray fluorescence analysis provided further evidence of heavy metal reduction with significant decreases in metal concentrations: Cr (from 14.0 to 3.09 ppm), Mn (15.5 to 5.11 ppm), Pb (5.8 to 3.09 ppm), and Ni (5.0 to 2.88 ppm). These results not only confirm the effectiveness of the treatment process under optimal conditions but also demonstrate the potential for significantly reducing the environmental hazards associated with PG, thus enhancing its potential for reuse or safer disposal.

Fourier transform infrared spectroscopy confirmed that the structural integrity of PG was largely retained following treatment. Key functional groups characteristic of PG, including O–H and SO_4^{2-} vibrational bands, remained identifiable post-treatment, indicating that Na_2EDTA does not induce significant degradation of the PG matrix. This finding supports the feasibility of using Na_2EDTA without compromising the mineralogical identity of PG.

X-ray diffraction analysis offered significant information on the mineralogical alterations within the PG structure. The

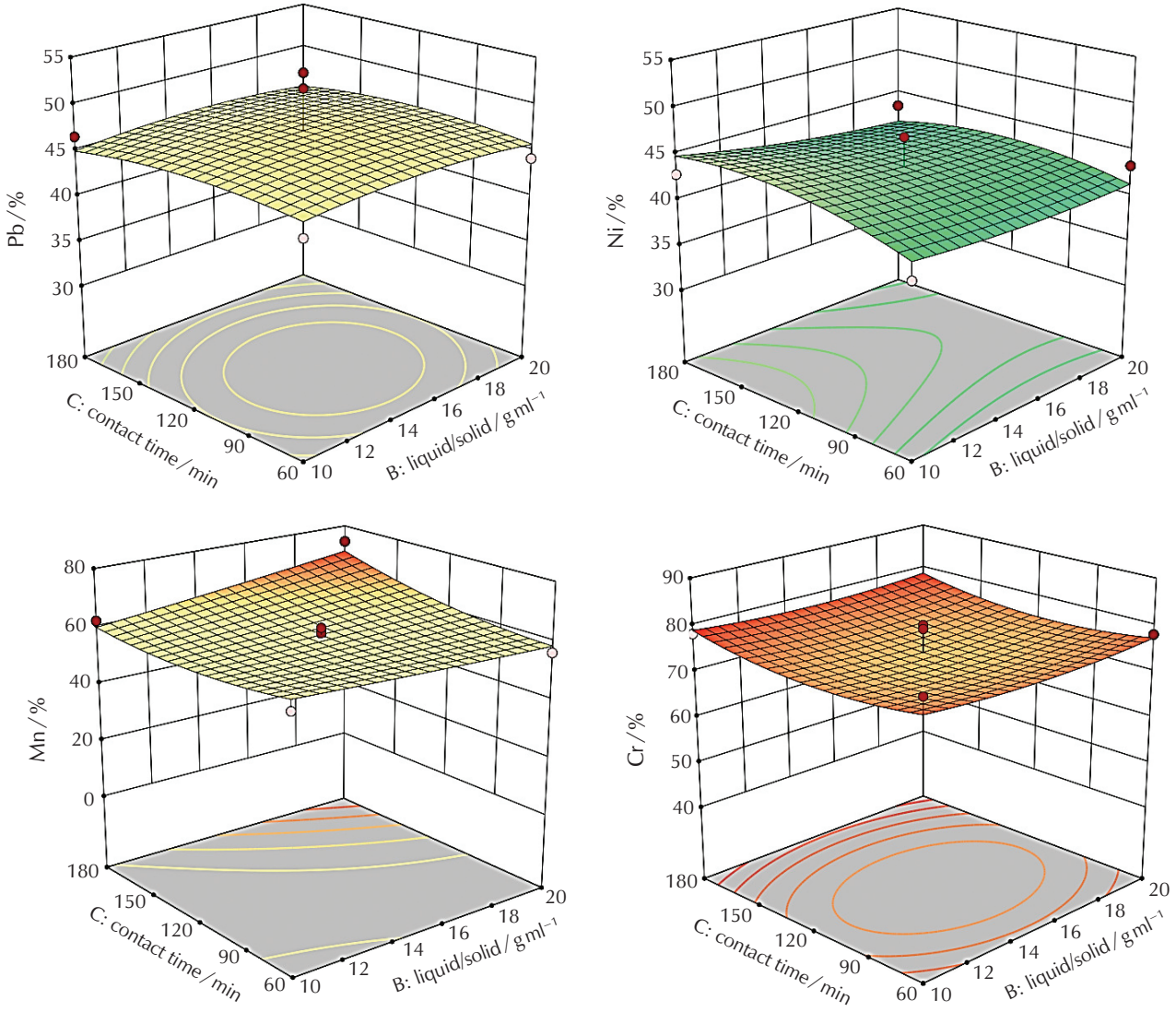

Fig. 8 – Response surface plots of contact time and solid-to-liquid ratio

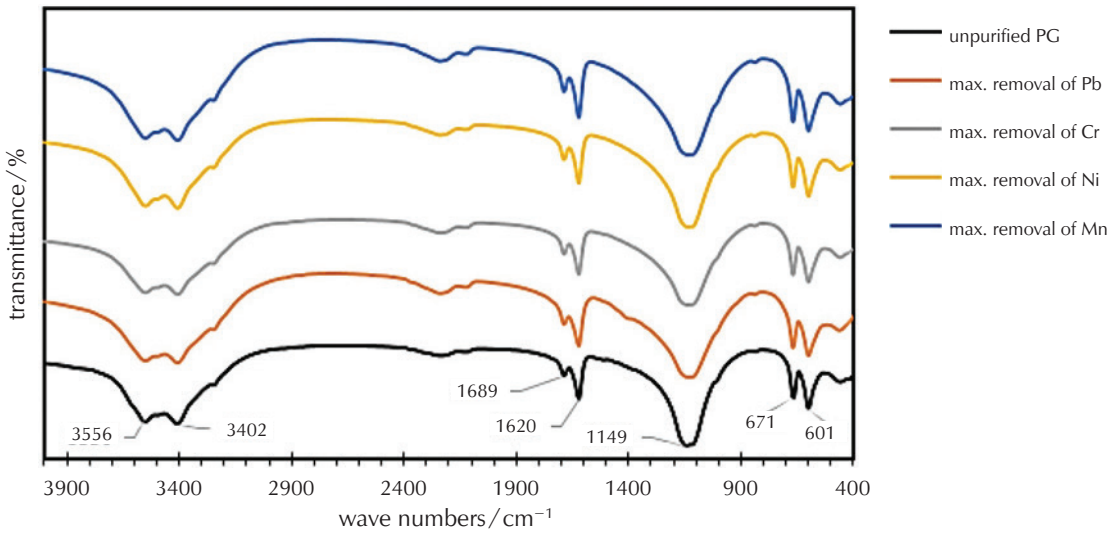

Fig. 9 – FTIR spectra of phosphogypsum unpurified and after purification

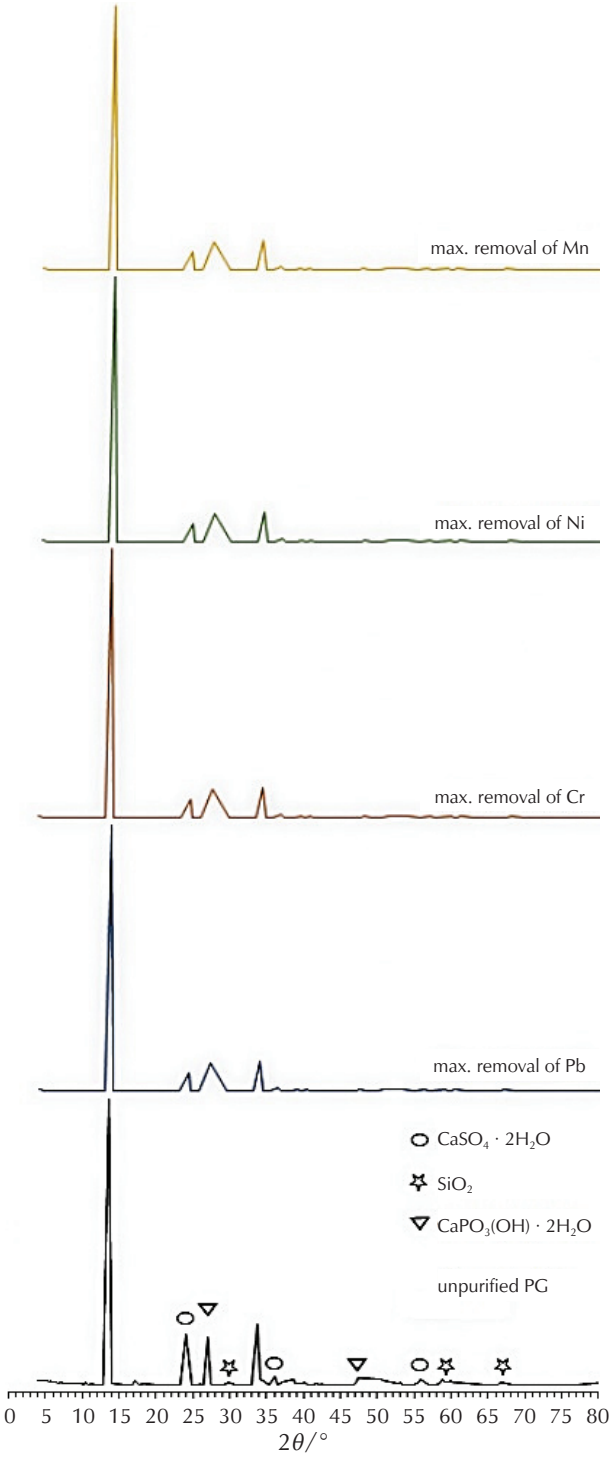

Fig. 10 – XRD spectrum of phosphogypsum unpurified and after purification

dominant presence of calcium sulphate dihydrate along with traces of brushite and quartz was noted in the untreated sample. Post-treatment patterns indicated partial dissolution of phases, particularly involving calcium compounds, suggesting that Na_2EDTA interacts primarily with metal-associated fractions rather than the bulk PG matrix.

Given the environmental concerns related to the persistence of EDTA in ecosystems, the recovery and reuse of

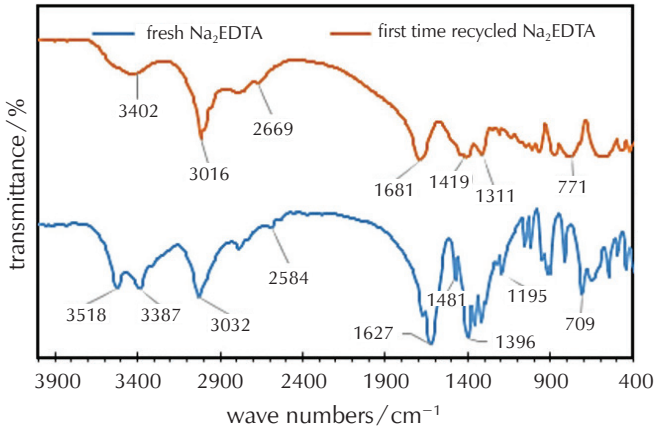

Fig. 11 – FTIR spectrum of fresh Na_2EDTA and first-time recycled Na_2EDTA

Na_2EDTA were also explored. A precipitation method using sulphuric acid successfully recovered 71.4 % of the chelating agent. FTIR spectra of the recovered Na_2EDTA showed strong similarities with fresh Na_2EDTA, particularly in key functional groups associated with carboxyl and hydroxyl regions, confirming that the recovered compound maintains its chemical integrity and remains suitable for reuse.

In summary, this study demonstrates that Na_2EDTA is an effective, structurally compatible and recoverable chelating agent for the simultaneous removal of multiple heavy metals from PG. The optimised treatment parameters provide a reproducible and efficient approach for reducing heavy metal content in PG, thereby lowering its environmental impact and enhancing its potential for sustainable reuse. Future studies may focus on improving the recovery efficiency of Na_2EDTA and assessing the long-term environmental behaviour of the treated PG in various application scenarios.

ACKNOWLEDGEMENTS

This study was financially supported by the Scientific and Technological Research Council of Turkey (TÜBİTAK, Project No: 118C085) and conducted with the cooperation of Ankara University and Toros Agri R&D Center within the scope of TÜBİTAK 2244 Industrial PhD Fellowship Programme. The authors would like to thank the Earth Sciences Application and Research Center (YEBİM) from Ankara University for XRF and XRD analyses.

List of abbreviations

ANOVA – analysis of variance
BBD – Box-Behnken Design
EDTA – ethylenediamine tetra acetic acid
EPA – Environmental Protection Agency
PTEs – essential and potentially toxic elements
RSM – response surface methodology

References
Literatura

1. *P. M. Rutherford, M. J. Dudas, R. A. Samek,* Environmental impacts of phosphogypsum, Sci. Total Environ. **149** (1-2) (1994) 1–38, doi: https://doi.org/10.1016/0048-9697(94)90002-7.
2. *L. Yang, Y. Yan, Z. Hu,* Utilization of phosphogypsum for the preparation of non-autoclaved aerated concrete, Constr. Build. Mater. **44** (2013) 600–606, doi: https://doi.org/10.1016/j.conbuildmat.2013.03.070.
3. *M. Contreras, S. R. Teixeira, G. T. A. Santos, M. J. Gázquez, M. Romero, J. P. Bolívar,* Influence of the addition of phosphogypsum on some properties of ceramic tiles, Constr. Build. Mater. **175** (2018) 588–600, doi: https://doi.org/10.1016/j.conbuildmat.2018.04.131.
4. *K. Gijbels, Y. Pontikes, R. I. Iacobescu, S. Schreurs, W. Schroeyers, T. Kuppens,* Techno-economic and environmental analysis of alkali-activated materials containing phosphogypsum and blast furnace slag, in: Sustainability Assessments for the Low Carbon Economy, Interdisciplinary PhD Expert Course for Young Researchers, Hasselt, Belgium, 2017.
5. *J. B. Carmichael,* Worldwide production and utilization of PG, in: Proceedings of the Second International Symposium on PG, 1988, 01-037-055 105-110.
6. *H. Hassoune, A. Lachehab, K. E. Hajjaji, O. Mertah, A. Kherbeche,* Dynamic of Heavy Metals and Environmental Impact of Waste Phosphogypsum, in: P. K. Gupta, R. N. Bharagava, (eds), Fate and Transport of Subsurface Pollutants, Vol. **24**, 2021, Springer, Singapore, pp. 57–77, doi: https://doi.org/10.1007/978-981-15-6564-9_4.
7. *A. H. T. Kandil, M. F. Cheira, H. S. Gado, M. H. Soliman, H. M. Akl,* Ammonium sulfate preparation from phosphogypsum waste, J. Radiat. Res. Appl. Sci. **10** (1) (2017) 24–33, doi: https://doi.org/10.1016/j.jrras.2016.11.001.
8. *Y. Chernysh, O. Yakhnenko, V. Chubur, H. Roubík,* Phosphogypsum recycling: a review of environmental ıssues, current trends, and prospects, Appl. Sci. **11** (4) (2021) 1575, doi: https://doi.org/10.3390/app11041575.
9. *M. Villa, F. Mosqueda, S. Hurtado, J. Mantero, G. Manjón, R. Periañez, F. Vaca, R. García-Tenorio,* Contamination and restoration of an estuary affected by phosphogypsum releases, Sci. Total Environ. **408** (1) (2009) 69–77, doi: https://doi.org/10.1016/j.scitotenv.2009.09.028.
10. *M. A. Nadymova*, Apatite concentrate as a promising source of rare-earth metals in complex processing, in: The North and the Arctic in the New Global Development Paradigm, Luzin Readings, Proceedings of the International Scientific and Practical Conference, Apatity, Russia, 2016, pp. 674–679.
11. *L. L. Tovazhnyansky, V. P. Meshalkin, P. O. Kapustenko, S. I. Bukhkalo, O. P. Arsenyeva, O. Y. Perevertaylenko*, Energy efficiency of complex technologies of phosphogypsum conversion, Theor. Found Chem. Eng. **47** (3) (2013) 225–230, doi: https://doi.org/10.1134/S0040579513030135.
12. *L. Reijnders,* Cleaner phosphogypsum, coal combustion ashes and waste incineration ashes for application in building materials, A review, Build. Environ. **42** (2) (2007) 1036–1042, doi: https://doi.org/10.1016/j.buildenv.2005.09.016.
13. *O. Hentati, N. Abrantes, A. L. Caetano, S. Bouguerra, F. Gonçalves, J. Römbke, R. Pereira,* Phosphogypsum as a soil fertilizer: Ecotoxicity of amended soil and elutriates to bacteria, invertebrates, algae and plants, J. Hazard. Mater. **294** (2015) 80–89, doi: https://doi.org/10.1016/j.jhazmat.2015.03.034.
14. *S. Nayak, C. S. K. Mishra, B. C. Guru, M. Rath*, Effect of phosphogypsum amendment on soil physico-chemical properties, microbial load and enzyme activities, J. Environ. Biol. **32** (5) (2011) 613–617.
15. *J. Yang, F. Lv, J. Zhou, Y. Song, F. Li,* Health risk assessment of vegetables grown on the contaminated soils in Daye City of Hubei Province, China, Sustainability **9** (11) (2017) 2141, doi: https://doi.org/10.3390/su9112141.
16. *M. Singh, M. Garg, C. L. Verma, S. K. Handa, R. Kumar,* An improved process for the purification of phosphogypsum, Constr. Build. Mater. **10** (8) (1996) 597–600, doi: https://doi.org/10.1016/S0950-0618(96)00019-0.
17. *M. Singh,* Treating waste phosphogypsum for cement and plaster manufacture, Cem. Concr. Res. **32** (7) (2022) 1033–1038, doi: https://doi.org/10.1016/S0008-8846(02)00723-8.
18. *A. Jarosinski, J. Kowalczyk, C. Mazanek*, Development of the Polish wasteless technology of apatite phosphogypsum utilization with recovery of rare-earths, J. Alloys Compd. **200** (1-2) (1993) 147–150, doi: https://doi.org/10.1016/0925-8388(93)90485-6.
19. *R. S. Tejowulan, W. H. Hendershot,* Removal of trace metals from contaminated soils using EDTA incorporating resin trapping techniques, Environ. Pollut. **103** (1) (1998) 135–142, doi: https://doi.org/10.1016/S0269-7491(98)00080-3.
20. *M. Udovic, D. Lestan,* EDTA Leaching of Cu Contaminated Soils Using Ozone/UV for Treatment and Reuse of Washing Solution in a Closed Loop, Water Air Soil Poll. **181** (2007) 319–327, doi: https://link.springer.com/article/10.1007/s11270-006-9304-x.
21. *M. Udovic, D. Lestan,* EDTA and HCl leaching of calcareous and acidic soils polluted with potentially toxic metals: remediation efficiency and soil impact, Chemosphere **88** (6) (2012) 718–724, doi: https://doi.org/10.1016/j.chemosphere.2012.04.040.
22. *T. Sun, J. Beiyuan, G. Gielen, X. Mao, Z. Song, S. Xu, Y. S. Ok, J. Rinklebe, D. Liu, D. Hou, J. W. C. Wong, H. Wang,* Optimizing extraction procedures for better removal of potentially toxic elements during EDTA-assisted soil washing, J. Soils Sediments **20** (2020) 3417–3426, doi: https://doi.org/10.1007/s11368-020-02678-0.
23. *M. Cheikh, J. P. Magnin, N. Gondrexon, J. Willison, A. Hassen,* Zinc and lead leaching from contaminated industrial waste sludges using coupled processes, Environ. Technol. **31** (14) (2010) 1577–1585, doi: https://doi.org/10.1080/09593331003801548.
24. *S. Gitipour, S. Ahmadi, E. Madadian, M. Ardestani,* Soil washing of chromium- and cadmium-contaminated sludge using acids and ethylenediaminetetra acetic acid chelating agent, Environ. Technol. **3** (1) (2016) 145–151, doi: https://doi.org/10.1080/09593330.2011.597784.
25. *D. Pant, P. Singh, M. K. Upreti,* Metal leaching from cathode ray tube waste using combination of *Serratia plymuthica* and EDTA, Hydrometallurgy **146** (2014) 89–95, doi: https://doi.org/10.1016/j.hydromet.2014.02.016.
26. *M. Bilgin, S. Tulun,* Removal of heavy metals (Cu, Cd and Zn) from contaminated soils using EDTA and $FeCl_3$, Glob. Nest. J. **18** (1) (2016) 98–107, doi: https://doi.org/10.30955/gnj.001732.
27. *D. Voglar, D. Lestan,* Chelant soil-washing technology for metal-contaminated soil, Environ. Technol. **35** (11) (2014) 1389–400, doi: https://doi.org/10.1080/09593330.2013.869265.
28. *G. D. Christian, P. K. Dasgupta, K. A. Schug,* Analytical Chemistry, 7th Edition, Wiley, New York, 2015, pp. 322–341.
29. *G. Tan, Q. Liu, X. Li, Y. Liu, D. Xiao,* Porous carbon material prepared from Na_2EDTA and its performance in capacitive

deionization process, Appl. Surf. Sci. **496** (2019) 143526, doi: https://doi.org/10.1016/j.apsusc.2019.07.268.

30. *A. Raheem, L. Ding, Q. He, F. H. Mangi, Z. H. Khand, M. Sajid, A. Ryzhkov, G. Yu,* Effective pretreatment of corn straw biomass using hydrothermal carbonization for co-gasification with coal: Response surface Methodology–Box Behnken design, Fuel **324** (2022) 124544, doi: https://doi.org/10.1016/j.fuel.2022.124544.
31. *S. Mondal, K. Aikat, G. Halder,* Biosorptive uptake of arsenic(V) by steam activated carbon from mung bean husk: equilibrium, kinetics, thermodynamics and modeling, Appl. Water Sci. **7** (2017) 4479–4495, doi: https://link.springer.com/article/10.1007/s13201-017-0596-3.
32. *S. M. Samuel, M. E. A. Abigail, R. Chidambaram,* Isotherm modelling, kinetic study and optimization of batch parameters using response surface methodology for effective removal of Cr(VI) using fungal biomass, PLoS One **10** (2015) 1–15, doi: https://doi.org/10.1371/journal.pone.0116884.
33. *M. Al-Hwaiti, J. Ranville, P. Ross,* Bioavailability and mobility of trace metals in phosphogypsum from Aqaba and Eshidiya, Jordan, Geochemistry **70** (3) (2010) 283–291, doi: https://doi.org/10.1016/j.chemer.2010.03.001.
34. *H. Song, H. Chung, K. Nam,* Response surface modeling with Box-Behnken design for strontium removal from soil by calcium-based solution, Environ. Pollut. **274** (2021), doi: https://doi.org/10.1016/j.envpol.2021.116577.
35. *S. Y. Guvenc, G. Varank,* Box-Behnken design optımızatıon of electro-fenton/-persulfate processes followıng the acıdıfıcatıon for tss removal from bıodıesel wastewater, Sigma J. Eng. Nat. Sci. **38** (4) (2020) 1767–1780, doi: https://dergipark.org.tr/en/pub/sigma/issue/65287/1004983.
36. *A. E. Shahawy, R. H. Mohamadien, E. M. El-Fawal, Y. M. Moustafa, M. M. K. Dawood,* Hybrid Photo-Fenton oxidation and biosorption for petroleum wastewater treatment and optimization using Box–Behnken Design, Environ. Technol. Inno. **24** (2021), doi: https://doi.org/10.1016/j.eti.2021.101834.
37. *A. Reghioua, D. Barkat, A. H. Jawad, A. S. Abdulhameed, A. A. Al-Kahtani, Z. A. ALOthman,* Parametric optimization by Box–Behnken design for synthesis of magnetic chitosan-benzil/ZnO/Fe_3O_4 nanocomposite and textile dye removal, J. Environ. Chem. Eng. **9** (3) (2021), doi: https://doi.org/10.1016/j.jece.2021.105166.
38. *P. Vitale, P. B. Ramos, V. Colasurdo, M. B. Fernandez, G. N. Eyler,* Treatment of real wastewater from the graphic industry using advanced oxidation technologies: Degradation models and feasibility analysis, J. Clean Prod. **206** (2019) 1041–1050, doi: https://doi.org/10.1016/j.jclepro.2018.09.105.
39. *J. Segurola, N. S. Allen, M. Edge, A. M. Mahon,* Design of eutectic photoinitiator blends for UV/visible curable acrylated printing inks and coatings, Prog. Org. Coat. **37** (1-2) (1999) 23–37, doi: https://doi.org/10.1016/S0300-9440(99)00052-1.
40. *J. Qu, X. Meng, H. You, X. Yei, Z. Du,* Utilization of rice husks functionalized with xanthates as cost-effective biosorbents for optimal Cd(II) removal from aqueous solution *via* response surface methodology, Bioresour. Technol. **241** (2017) 1036–1042, doi: https://doi.org/10.1016/j.biortech.2017.06.055.
41. *U. K. Sahu, M. K. Sahu, S. S. Mahapatra, R. K. Patel,* Removal of As(III) from aqueous solution using Fe_3O_4 nanoparticles: process modeling and optimization using statistical design, Water Air Soil Pollut. **228** (2017) 1–15, doi: https://link.springer.com/article/10.1007/s11270-016-3224-1.
42. *W. Yuana, J. Chenga, H. Huangb, S. Xiong, J. Gao, J. Zhang S. Feng,* Optimization of cadmium biosorption by Shewanella putrefaciens using a Box-Behnken design, Ecotoxicol Environ. Saf. **175** (2019) 138–147, doi: https://doi.org/10.1016/j.ecoenv.2019.03.057.
43. *S. Saha, B. H. Jeon, M. B. Kurade, S. B. Jadhav, P. K. Chatterjee, S. W. Chang, S. P. Govindwar, S. J. Kim,* Optimization of dilute acetic acid pretreatment of mixed fruit waste for increased methane production, J. Clean. Pro. **190** (2018) 411–421, doi: https://doi.org/10.1016/j.jclepro.2018.04.193.
44. *E. Natarajan, G. P. Ponnaiah,* Optimization of process parameters for the decolorization of Reactive Blue 235 dye by barium alginate immobilized iron nanoparticles synthesized from aluminum industry waste, Environ. Nanotechnol. Monit. Manag. **7** (2017) 73–88, doi: https://doi.org/10.1016/j.enmm.2017.01.002.
45. *T.* Ölmez, The optimization of Cr(VI) reduction and removal by electrocoagulation using response surface methodology, J. Hazard. Mater. **162** (2009) 1371–1378, doi: https://doi.org/10.1016/j.jhazmat.2008.06.017.
46. *M. R. Hadiani, K. K. Darani, N. Rahimifard, H. Younesi,* Biosorption of low concentration levels of Lead (II) and Cadmium (II) from aqueous solution by *Saccharomyces cerevisiae*: Response surface methodology, Biocatal. Agric. Biotechnol. **15** (2018) 25–34, doi: https://doi.org/10.1016/j.bcab.2018.05.001.
47. *A. Choińska-Pulita, J. Sobolczyk-Bednareka, W.* Łaba, Optimization of copper, lead and cadmium biosorption onto newly isolated bacterium using a Box-Behnken design. Ecotoxicol. Environ. Saf. **149** (2018) 275–283, doi: https://doi.org/10.1016/j.ecoenv.2017.12.008.
48. *Y. Chernysh, M. Balintova, L. Plyatsu, M. Holub, S. Demcak,* The influence of phosphogypsum addition on phosphorus release in biochemical treatment of sewage sludge, Int. J. Environ. Res. Public Health **15** (6) (2018) 1269, doi: https://doi.org/10.3390/ijerph15061269.
49. *X. Mu, G. Zhu, X. Li, S. Li, X. Gong, H. Li, G. Sun,* Effects of impurities on $CaSO_4$ crystallization in the $Ca(H_2PO_4)_2$–H_2SO_4–H_3PO_4–H_2O system, ACS omega **4** (7) (2019) 12702–12710, doi: https://doi.org/10.1021/acsomega.9b01114.
50. *H. Wu, P, Wang, Z. Wang, Z. Sun Y, C. Li, Y. Dong,* Preparation of EDTA modified cotton fiber iron complex and catalytic properties for aqueous Cr (VI) reduction and dye degradation, Water Pract. Technol. **16** (3) (2021) 1000–1011, doi: https://doi.org/10.2166/wpt.2021.047.
51. *J. Beiyuan, D. C. Tsang, M. Valix, K. Baek, Y. S. Ok, W. Zhang, N. S. Bolan, J. Rinklebe, X. D. Li,* Combined application of EDDS and EDTA for removal of potentially toxic elements under multiple soil washing schemes, Chemosphere **205** (2018) 178–187, doi: https://doi.org/10.1016/j.chemosphere.2018.04.081.
52. *R. W. Peters,* Chelant extraction of heavy metals from contaminated soil, J. Hazard. Mater. **66** (1-2) (1999) 151–210, doi: https://doi.org/10.1016/S0304-3894(99)00010-2.
53. *S. Goel, K. K. Pant, K. D. P. Nigam,* Extraction of nickel from spent catalyst using fresh and recovered EDTA, J. Hazard. Mater. **171** (1-3) (2009) 253–261, doi: https://doi.org/10.1016/j.jhazmat.2009.05.131.
54. *K. C. Lanigan, K. Pidsosny,* Reflectance FTIR spectroscopic analysis of metal complexation to EDTA and EDDS, Vib. Spectros. **4** (1) (2007) 2–9, doi: https://doi.org/10.1016/j.vibspec.2007.03.003.

SAŽETAK

Istodobno uklanjanje Pb, Ni, Mn i Cr iz fosfogipsa pomoću Na_2EDTA: optimizacija i modeliranje primjenom Box-Behnkenovog dizajna

Ertuğrul Çelik[a,b*] i *Suna Ertunç*[a*]

Fosfogips (PG) smatra se nusproizvodom fosforne kiseline nastale reakcijom sumporne kiseline s fosfatnom rudom mokrim postupkom, a klasificira se kao kruti otpad. Prisutnost teških metala u PG-u uzrokuje niz ekoloških problema te ograničava njegovu moguću primjenu. U ovom istraživanju primijenjen je Box-Behnkenov dizajn (BBD) s ciljem optimizacije uklanjanja olova, nikla, mangana i kroma u PG-u pomoću Na_2EDTA. U tu svrhu optimizirali su se čimbenici poput koncentracije Na_2EDTA, omjera kruto/tekuće (S/L) i kontaktnog vremena, uz istodobni razvoj matematičkog modela. Optimalne procesne točke identificirane su analizom varijance (ANOVA) i grafikonima odzivne površine. Nadalje, fizikalno-kemijska svojstva PG-a prije i nakon pročišćavanja analizirana su tehnikama XRF, XRD i FTIR. Na temelju rezultata dobivenih metodologijom odzivnih površina, koeficijenti korelacije (R^2) eksperimentalnih podataka i regresijskog modela drugog reda za Pb, Ni, Mn i Cr iznosili su 89,75, 95,37, 98,18 i 94,53 %. Općenito, visoke vrijednosti R^2 upućuju na to da se eksperimentalni podatci slažu s podatcima predviđenima modelom pri optimalnim uvjetima: $c(Na_2EDTA)$ = 0,055 M, omjer kruto/tekuće = 1 : 20 g ml^{-1}, kontaktno vrijeme = 157 min. U tim uvjetima, učinkovitosti uklanjanja Pb, Ni, Mn i Cr iznosile su 46,65, 42,31, 67,02 i 77,9 %.

Ključne riječi
Fosfogips, Na_2EDTA, uklanjanje teških metala, dizajn eksperimenta Box-Behnken

[a] *Ankara University, Department of Chemical Engineering, 06100 Ankara, Turska*
[b] *Toros Agri Industry and Trade Co. Inc. R&D Center, 33 020 Mersin, Turska*

Izvorni znanstveni rad
Prispjelo 22. veljače 2025.
Prihvaćeno 16. travnja 2025.